

An epidemiological model for West Nile virus: invasion analysis and control applications

Marjorie J. Wonham^{1,2,3*}, Tomás de-Camino-Beck¹ and Mark A. Lewis^{1,2}

¹Department of Biological Sciences, and ²Department of Mathematical and Statistical Sciences, University of Alberta, Edmonton, Alberta T6G 2G1, Canada

³Great Lakes Institute for Environmental Research, University of Windsor, Windsor, Ontario N9B 3P4, Canada

Infectious diseases present ecological and public health challenges that can be addressed with mathematical models. Certain pathogens, however, including the emerging West Nile virus (WN) in North America, exhibit a complex seasonal ecology that is not readily analysed with standard epidemiological methods. We develop a single-season susceptible–infectious–removed (SIR) model of WN cross-infection between birds and mosquitoes, incorporating specific features unique to WN ecology. We obtain the disease reproduction number, R_0 , and show that mosquito control decreases, but bird control increases, the chance of an outbreak. We provide a simple new analytical and graphical method for determining, from standard public health indicators, necessary mosquito control levels. We extend this method to a seasonally variable mosquito population and outline a multi-year model framework. The model's numerical simulations predict disease levels that are consistent with independent data.

Keywords: arbovirus; emerging infectious disease; outbreak threshold; public health; reproduction number

1. INTRODUCTION

Emerging infectious diseases are a growing agent of global change that present compelling challenges in public health, agriculture and wildlife management (Blower & McLean 1991; Binder *et al.* 1999; Keeling *et al.* 2001). Arthropod-borne diseases including West Nile virus (WN) provide unique opportunities to explore the ecological links between host and vector species. Translating this ecology into a dynamic model allows the evaluation of different control strategies (Anderson & May 1991). At the same time, however, a biologically realistic model of seasonal host–vector cross-infection is necessarily complicated and not necessarily amenable to classical analysis. As we show here, the application of new graphical methods can simplify the calculation of threshold parameters controlling disease outbreak.

We focus on the emerging WN epidemic in North America, which has been exceptionally well documented at both host and vector levels. The virus is widespread in Africa, the Middle East and western Asia, with occasional European outbreaks introduced by migrating birds (Hayes 1988; Rappole *et al.* 2000). In North America, the first recorded epidemic was initially detected in New York state in 1999 and spread rapidly across the continent causing unprecedented bird, horse and human mortality attributed to a highly virulent emerging virus strain (Anderson *et al.* 1999; Petersen & Roehrig 2001). Control strategies focus primarily on the eradication of vector mosquitoes (New York City 2003). We develop the simplest possible biologically relevant ordinary differential equations model for WN transmission, obtain the disease basic reproduction number R_0 (Anderson & May 1991), determine outbreak criteria and graphically relate virus detection and control metrics.

2. MODEL DESCRIPTION

Like many arboviruses, WN persists in natural transmission cycles between vectors (mosquitoes) and reservoir hosts (birds). Mammals are secondary hosts generally considered unimportant to disease persistence in the wild (Hayes 1988). We therefore focused only on cross-infection between birds and mosquitoes. Understanding this simplified system has clear implications for disease management in mammalian hosts, including humans.

To account for time-scales specific to WN, we extended the classical SIR differential-equation model for malaria transmission (Anderson & May 1991; Thomas & Urena 2001) to an eight-compartment model describing WN cross-infection in one season (figure 1). The dimensional equations for this dynamic system (equations (2.1)) describe susceptible (S_B), infectious (I_B), recovered (R_B) and dead (X_B) birds, where the total live bird population is $N_B = (S_B + I_B + R_B)$, and larval (L_M), susceptible (S_M), exposed (E_M) and infectious (I_M) female mosquitoes, where the total female mosquito population is $N_M = (L_M + S_M + E_M + I_M)$ (figure 1) (all parameters are defined in table 1):

$$\frac{dS_B}{dt} = -abI_M \frac{S_B}{N_B}, \quad (2.1a)$$

$$\frac{dI_B}{dt} = abI_M \frac{S_B}{N_B} - \mu_V I_B - gI_B, \quad (2.1b)$$

$$\frac{dR_B}{dt} = gI_B, \quad (2.1c)$$

$$\frac{dX_B}{dt} = \mu_V I_B, \quad (2.1d)$$

* Author for correspondence (mwonham@ualberta.ca).

$$\frac{dL_M}{dt} = \beta_M(S_M + E_M + I_M) - mL_M - \mu_L L_M, \quad (2.1e)$$

$$\frac{dS_M}{dt} = -acS_M \frac{I_B}{N_B} + mL_M - \mu_A S_M, \quad (2.1f)$$

$$\frac{dE_M}{dt} = acS_M \frac{I_B}{N_B} - kE_M - \mu_A E_M, \quad (2.1g)$$

$$\frac{dI_M}{dt} = kE_M - \mu_A I_M. \quad (2.1h)$$

The following WN-specific elements are, we believe, essential to capturing the disease dynamics. The larval mosquito class L_M encompasses all stages from egg to adult emergence (*ca.* 15 days), during which individuals are not involved in virus cross-infection. The exposed class, E_M , reflects the viral incubation period (*ca.* 8–12 days), which has been reported in mosquitoes but not birds (Senne *et al.* 2000; Langevin *et al.* 2001; Sardelis & Turell 2001; Swayne *et al.* 2001a,b; Turell *et al.* 2001). These two classes together can constitute 50–60% of the total mosquito lifespan in north-temperate populations. We omit a removed mosquito class since vectors are not known to respond to WN infection and their viraemia profile remains to be determined.

Cross-infection between birds and mosquitoes is modelled as mass-action kinetics normalized by bird density. This follows Anderson & May (1991) in assuming a saturated functional response of mosquito biting rate to bird density. The model considers a single season from spring to autumn, so vital dynamics are included for mosquitoes but not for birds. Disease mortality and recovery in birds, and vital dynamics in mosquitoes, are modelled as density independent. We further assume for this simple model that vertical transmission in mosquitoes and horizontal transmission in birds are negligible (*cf.* Langevin *et al.* 2001; McLean *et al.* 2001; Nasci *et al.* 2001; Turell *et al.* 2001).

YOU CAN SKIP THIS SECTION. START AGAIN AT EQ 3.5
3. MODEL ANALYSIS

To non-dimensionalize the WN system we scaled time, t , with the quantity $1/k$ by setting $\tau = kt$, scaled all parameters to k (table 1) and scaled bird and mosquito numbers by the initial bird population, N_{B0} . In the resulting dimensionless system (equations (3.1)), the four bird compartments, s_b, i_b, r_b and x_b , indicate the fractions of the initial population in the susceptible, infectious, recovered, and dead classes, respectively, where the total live bird population, n_b , is $0 \leq n_b = (s_b + i_b + r_b) \leq 1$. The four mosquito compartments, l_m, s_m, e_m and i_m represent larval, susceptible, exposed and infectious females, respectively, scaled to the initial number of birds, where the total female mosquito population, n_m , is $0 \leq n_m = (l_m + s_m + e_m + i_m)$. The rescaled system is

$$\frac{ds_b}{d\tau} = -\alpha_b i_m \frac{s_b}{n_b}, \quad (3.1a)$$

$$\frac{di_b}{d\tau} = \alpha_b i_m \frac{s_b}{n_b} - \mu_v i_b - \gamma i_b, \quad (3.1b)$$

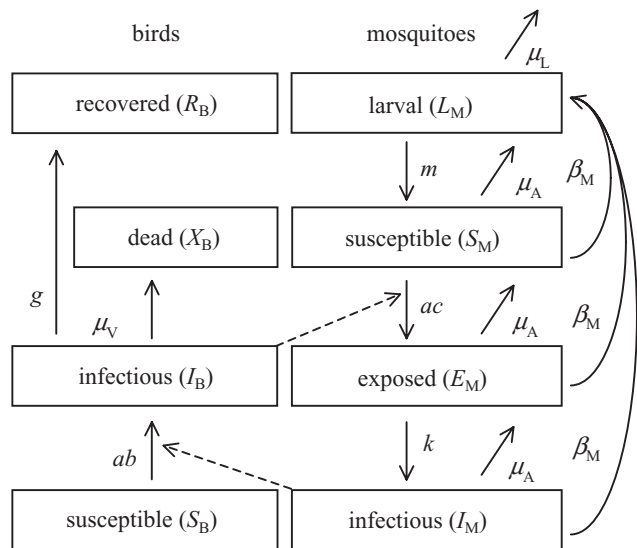


Figure 1. Compartment model for WN cross-infection between birds and mosquitoes. See table 1 for parameter descriptions.

$$\frac{dr_b}{d\tau} = \gamma i_b, \quad (3.1c)$$

$$\frac{dx_b}{d\tau} = \mu_v i_b, \quad (3.1d)$$

$$\frac{dl_m}{d\tau} = \phi_m(s_m + e_m + i_m) - \eta l_m - \mu_l l_m, \quad (3.1e)$$

$$\frac{ds_m}{d\tau} = -\alpha_m s_m \frac{i_b}{n_b} - \mu_a s_m + \eta l_m, \quad (3.1f)$$

$$\frac{de_m}{d\tau} = \alpha_m s_m \frac{i_b}{n_b} - \mu_a e_m - e_m, \quad (3.1g)$$

$$\frac{di_m}{d\tau} = e_m - \mu_a i_m. \quad (3.1h)$$

In the absence of disease, the bird equilibrium for this system is $(s_{b0}, i_{b0}, r_{b0}, x_{b0}) = (1, 0, 0, 0)$. For mosquitoes, we chose vital-rate parameter relationships to balance birth and death rates in the disease-free state. By setting equations (2.1e,f) and I_{B0} equal to zero, we obtained $\beta_M = \mu_A(m + \mu_L)/m$, which ensures the following steady-state relationship between larval and susceptible adult mosquitoes:

$$L_{M0} = \frac{\beta_M S_{M0}}{(m + \mu_L)}, \quad l_{m0} = \frac{\phi_m s_{m0}}{(\eta + \mu_l)}. \quad (3.2)$$

Thus, for any given initial density of adult mosquitoes, s_{m0} , the resulting disease-free equilibrium (DFE) is $(l_{m0}, s_{m0}, e_{m0}, i_{m0}) = (\phi_m s_{m0}/(\eta + \mu_l), s_{m0}, 0, 0)$.

To evaluate the invasibility of this system we followed van den Driessche & Watmough (2002) in using vector notation to rewrite the equations in which infections appear in terms of the difference between f_j , the rate of appearance of new infections in compartment j , and v_j , the rate of transfer of individuals into and out of compartment j by all other processes. Although infections arise in

Table 1. Parameters in WN model.

(Numerical estimates for bird (B) and mosquito (M) parameters in dimensional (rates are daily and probabilities are per bite) and dimensionless (rescaled by k) forms. Mean, range and biological interpretation given for dimensional form. Literature values extracted primarily for the American crow, *Corvus brachyrhynchos* Brehm, the bird that has suffered some of the highest mortality in the North American WN epidemic, and for the mosquito *Culex pipiens* spp., a major North American WN vector (Bernard *et al.* 2001; Spielman 2001). Sources: 1, Turell *et al.* 2000; 2, Turell *et al.* 2001; 3, Sardelis & Turell 2001; 4, Hayes & Hsi 1975; 5, Mpho *et al.* 2002; 6, Oda *et al.* 1999; 7, Walter & Hacker 1974; 8, Reisen & Siddiqui 1979; 9, Mogi *et al.* 1984; 10, Reisen *et al.* 1989; 11, Work *et al.* 1955; 12, McLean *et al.* 2001; 13, Komar *et al.* 2003.)

dimensional	mean (range)	interpretation (sources)	dimensionless
a	0.09 (0.03–0.16)	M per capita biting rate on crows ^a	—
b	0.88 (0.80–1.00)	WN transmission probability, M to B (1, 2, 3)	$\alpha_b = ab/k$
c	0.16 (0.02–0.24)	WN transmission probability, B to M (1, 2, 3)	$\alpha_m = ac/k$
β_M	0.537 (0.036–42.5)	M per capita birth rate (see § 3)	$\phi_m = \beta_M/k$
m	0.068 (0.051–0.093)	M per capita maturation rate, larvae to adults (4, 5)	$\eta = m/k$
μ_A	0.029 (0.016–0.070)	M adult per capita mortality rate (6, 7)	$\mu_a = \mu_A/k$
μ_L	1.191 (0.213–16.9)	M larval per capita mortality rate calculated from the proportion of individuals surviving from egg to adult emergence, $e = m/(m + \mu_L) = 0.054$ (range of 0.003–0.304) (8, 9, 10)	$\mu_l = \mu_L/k$
k	0.106 (0.087–0.125)	M per capita transition rate, exposed to infected (3)	—
μ_v	0.143 (0.125–0.200)	B per capita mortality rate from WN (11, 12, 13)	$\mu_v = \mu_v/k$
g	0	B per capita recovery rate from WN (11, 13)	$\gamma = g/k$

^a The New York City Audubon Society database (<http://www.nycas.org/>) lists 26 common passerines, swifts, doves and kingbird species breeding within the city limits. In annual counts from 1988–1989 to 1998–1999, American crows constituted *ca.* 27% (range of 9–48%) of these birds in six Audubon Society Christmas Bird Count database circles in the Brooklyn, Queens, Suffolk Co., Nassau Co. and Staten Island regions of New York (NYBR, NYCS, NYNN, NYQU, NYSN, NYSI) (<http://www.audubon.org/bird/cbc/>). If we assume that *Culex* spp. mosquitoes bite only birds, that 27% of bites are on crows and that a female bites once every three days (Alameda County Mosquito Abatement District; <http://www.mosquitoes.org/Mosquitoes/LifeCycle.html>), we obtain the mean biting rate.

START AGAIN HERE!

i_b, e_m and i_m , only progression from s_m to e_m is considered to be a new infection, progression from e_m to i_m is not:

$$\frac{d}{d\tau} \begin{bmatrix} i_b \\ e_m \\ i_m \end{bmatrix} = f - v = \begin{bmatrix} \alpha_b i_m s_b \\ n_b s_b \\ \alpha_m s_m i_b \\ n_b i_b \\ 0 \end{bmatrix} - \begin{bmatrix} \mu_v i_b + \gamma i_b \\ \mu_a e_m + e_m \\ -e_m + \mu_a i_m \end{bmatrix}. \quad (3.3)$$

The corresponding Jacobian matrices, \mathcal{F} and \mathcal{V} , describe the linearization of this reduced system about the DFE,

$$\mathcal{F} = \begin{bmatrix} 0 & 0 & \alpha_b \\ \alpha_m s_{m0} & 0 & 0 \\ 0 & 0 & 0 \end{bmatrix}, \quad \mathcal{V} = \begin{bmatrix} \mu_v + \gamma & 0 & 0 \\ 0 & \mu_a + 1 & 0 \\ 0 & -1 & \mu_a \end{bmatrix}, \quad (3.4)$$

and the disease basic reproduction number, R_0 , is given as the dominant eigenvalue of $\mathcal{F}\mathcal{V}^{-1}$ (Driessche & Watmough 2002):

$$R_0 = \sqrt{\frac{\alpha_b}{\mu_a} \frac{\alpha_m s_{m0} \left(\frac{1}{1 + \mu_a} \right)}{(\mu_v + \gamma)}}$$

$$= \sqrt{\frac{ab}{\mu_A} \frac{ac \frac{S_{M0}}{N_{B0}} \left(\frac{k}{k + \mu_A} \right)}{(\mu_v + g)}}. \quad (3.5)$$

R_0 is defined as the number of secondary infections deriving from a single primary infection in a population of susceptibles (Anderson & May 1991). When $R_0 < 1$ the DFE is locally stable; when $R_0 > 1$ it is locally unstable, and disease introduction leads to an outbreak.

The biological meaning of R_0 is readily interpreted from the dimensional parameters. The first term under the square root represents the disease R_0 from mosquitoes to birds as the transmission probability (ab) multiplied by the adult mosquito infectious lifespan ($1/\mu_A$). The second term represents R_0 from birds to mosquitoes as the transmission probability (ac) multiplied by the number of initially susceptible mosquitoes per bird (S_{M0}/N_{B0}) that survive the exposed period ($k/[k + \mu_A]$), multiplied by the bird's infectious lifespan ($1/[(\mu_v + g)]$). The product gives the total disease R_0 from vector to vector or from host to host. The square root represents the geometric mean R_0 for an average individual of both species combined. Mosquito birth, maturation and larval mortality rates indirectly influence R_0 through the steady-state condition for adult mosquito mortality (equation (3.2)). Setting $R_0 = 1$

returns the critical equilibrium mosquito level, s_m^* , above which the virus will invade a constant population of susceptible mosquitoes:

$$s_{m0} = \frac{\mu_a(1 + \mu_a)(\gamma + \mu_v)}{\alpha_b \alpha_m} = s_m^* \tag{3.6}$$

SKIP THIS SECTION. START AGAIN AT 4. Model predictions

We used linear analysis to calculate the disease growth rate for the seasonal model extension. For the DFE $(s_{b0}, i_{b0}, r_{b0}, x_{b0}, l_{m0}, s_{m0}, e_{m0}, i_{m0}) = (1, 0, 0, 0, (\phi_m s_{m0})/(\eta + \mu_l), s_{m0}, 0, 0)$, we defined small perturbations in each variable, $(\tilde{s}_b, \tilde{i}_b, \tilde{r}_b, \tilde{x}_b, \tilde{l}_m, \tilde{s}_m, \tilde{e}_m, \tilde{i}_m)$. The corresponding Jacobian matrix, \mathcal{J} (which reduces to five dimensions since the \tilde{s}_b, \tilde{r}_b and \tilde{x}_b terms decouple), describes the linearization with respect to $(\tilde{i}_b, \tilde{l}_m, \tilde{s}_m, \tilde{e}_m, \tilde{i}_m)$:

$$\mathcal{J} = \begin{bmatrix} -\mu_v - \gamma & 0 & 0 & 0 & \alpha_b \\ 0 & -\eta - \mu_l & \phi_m & \phi_m & \phi_m \\ -\alpha_m s_{m0} & \eta & -\mu_a & 0 & 0 \\ \alpha_m s_{m0} & 0 & 0 & -\mu_a - 1 & 0 \\ 0 & 0 & 0 & 1 & -\mu_a \end{bmatrix} \tag{3.7}$$

This yields the charactersitic polynomial in λ :

$$0 = \det(\mathcal{J} - \lambda I) = \lambda \left(\lambda + \mu_a + \frac{\eta \phi_m}{\mu_a} \right) (\lambda^3 + a_1 \lambda^2 + a_2 \lambda + a_3), \tag{3.8}$$

where I is the 5×5 identity matrix and $a_1 > 0, a_2 > 0$. The zero root of the fifth-order polynomial (equation (3.8)) comes from the steady-state condition (equation (3.2)) that makes the disease-free mosquito population $(\phi_m s_{m0}/(\eta + \mu_l), s_{m0}, 0, 0)$ is neutrally stable to changes in s_{m0} . For $a_3 > 0$, by the Routh–Hurwitz conditions, all roots of the cubic polynomial in equation (3.8) have negative real parts. The disease outbreak threshold is thus when $a_3 = 0$ or, equivalently, when zero is the largest eigenvalue of \mathcal{J} . In biological terms the threshold may be thought of as a disease growth rate of zero, which corresponds directly to the reproduction number $R_0 = 1$.

START AGAIN HERE!

4. MODEL PREDICTIONS

Numerical simulations illustrate the predicted course of a WN outbreak (figure 2). Using mean parameter values (table 1), we calculated that the critical initial mosquito population for a WN outbreak at the DFE is $s_{m0} > s_m^* = 4.6$ adult female mosquitoes per initial bird (range of 0.37–1614, using minimum and maximum parameter values and fixing $k = 0.106$). The exact value of s_m^* depends on parameter values. American crows die quickly from WN infection (high μ_a) and are not known to recover to immunity ($\gamma = 0$). Using estimates for species with lower μ_v or higher γ (Work *et al.* 1955; Hayes 1988; Rap-pole *et al.* 2000; Bernard *et al.* 2001; Langevin *et al.* 2001; Komar *et al.* 2003) would decrease or increase s_m^* , respectively.

We compared our model predictions with disease prevalence data from the New York WN epidemic in 2000, using mean parameter values. For crows, public health data reported the proportion, p , of dead individuals that tested positive for WN ($p = 0.23$ – 0.67 ; Bernard *et al.*

2001). Although our model omits bird vital dynamics, we can estimate p as follows. Assuming a 4 year crow lifespan in the wild and a season of 14τ days ($\tau = 9.4$) where the final proportion of dead birds is x_{b14} , and assuming that WN-infected birds do not die of natural causes, we estimate $p = x_{b14}/[x_{b14} + 0.25(1 - x_{b14})]$. Given low, medium and high initial mosquito levels, the model predicts that 13%, 46% and 96% of crows die from the virus (x_{b14} in figure 2*a,c,e*), yielding $p = 0.37, 0.77$ and 0.99 . The two lower predictions overlap and the third is well above the reported range.

For infectious mosquitoes, the model predicts peak disease prevalences of $(i_m/n_m)_{\max} = 0.002, 0.01$ and 0.02 for the three initial levels in figure 2*b,d,f*. The two lower predictions encompass the reported range for vectors *Culex pipiens* and *C. pipiens-restuans* (0.004–0.0075; Bernard *et al.* 2001); the third is somewhat above this range. These results indicate that the lower s_{m0} values of the first two simulations (figure 2*a–d*) are more representative of the New York 2000 outbreak dynamics than that of the third (figure 2*e–f*). Further empirical data collection will allow more detailed model sensitivity analysis.

5. PUBLIC HEALTH IMPLICATIONS

Public health programmes currently use dead-crow density as a WN outbreak indicator (CDC 2002; New York City 2003). Model simulations show that dead-crow numbers increase much faster than numbers of live infected birds or infected mosquitoes (figure 2), which confirms that, logistics aside, monitoring dead crows is most effective in identifying an outbreak (unless of course WN immunity were to develop).

Although public health surveillance uses dead crows, our model uses the mosquito-to-crow ratio (s_{m0}) as a WN indicator. The two metrics can be related by using repeated numerical simulations to obtain a relationship between s_{m0} and the resulting crow survival (figure 3*a*). For a given season, s_{m0} can then be inferred from the observed loss of crows. For future seasons, the desired mosquito control level can be calculated (figure 3*a*), and the subsequent decrease in disease prevalence will reduce the infection risk for all hosts.

Current WN control targets mosquitoes (New York City 2003). The nonlinear relationship between s_m^* and μ_a (equation (3.6)) illustrates that a small increase in mosquito mortality can lead to a disproportionately large increase in the outbreak threshold. By contrast, reducing crow densities would be expected to enhance disease transmission (unless very low densities limited mosquito biting rates) since R_0 scales positively with the mosquito-to-bird ratio (equation (3.5)). For New York in 2000 (figure 2*a–d*), a 40–70% reduction of the initial mosquito population, i.e. reducing s_{m0} from 7.5–15 to less than 4.6, would have prevented the WN outbreak. Bird control, however, would have had the opposite effect.

6. TEMPORAL EXTENSIONS

We consider both within- and between-season extensions. Although the effects of continuous mosquito fluctuations could be computed numerically, we employed a discrete seasonality that permits analytical results and a

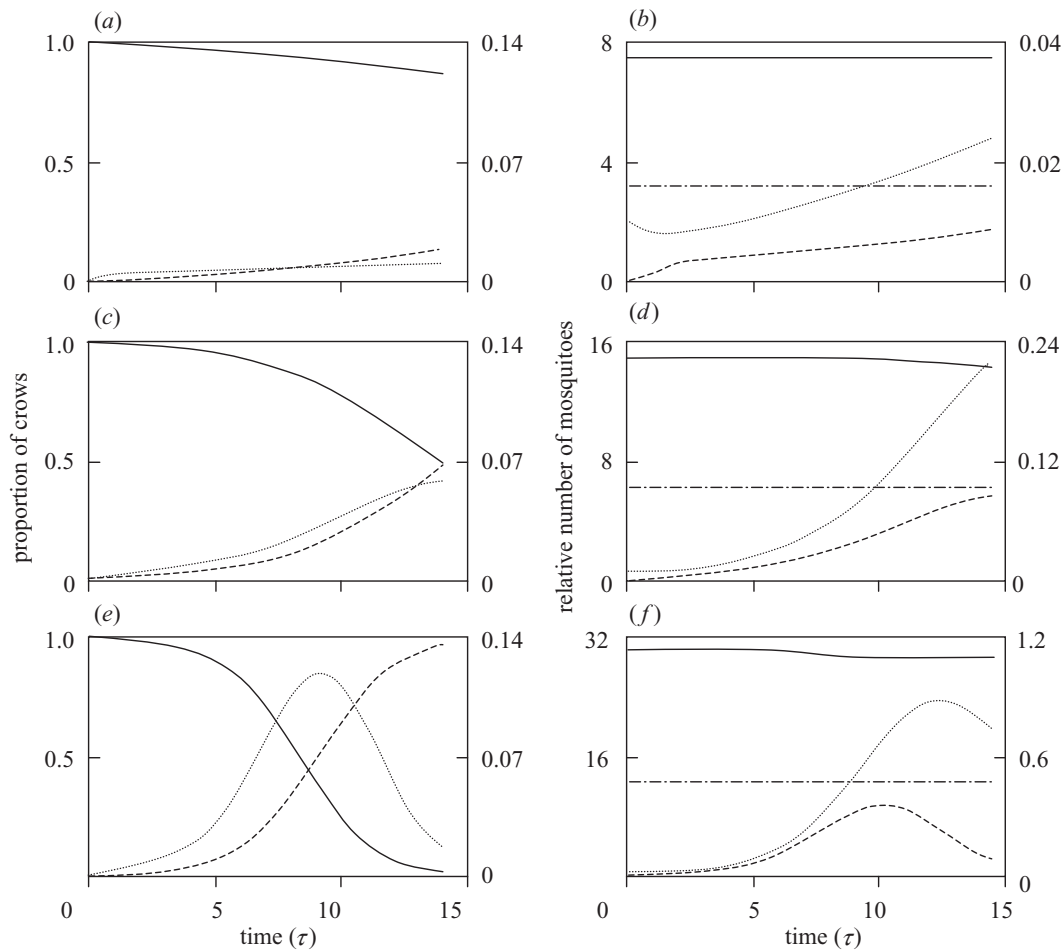


Figure 2. Numerical simulations of the proportions of crows (*a,c,e*) and relative numbers of mosquitoes (*b,d,f*) predicted by WN model for a steady-state mosquito population over a season lasting 14τ days. (*a,c,e*) The proportions of susceptible (s_b , solid line) and dead (x_b , dashed line) birds on the left axis and infectious birds (i_b , dotted line) on the right. (*b,d,f*) The relative numbers of susceptible (s_m , solid line) and larval (l_m , dot-dashed line) mosquitoes on the left axis and exposed (e_m , dashed line) and infectious (i_m , dotted line) mosquitoes on the right. A small addition of infected mosquitoes to a disease-free system ($i_{m0} = 0.01$) amplifies (*a,b*) to a mild outbreak when the initial level of susceptible mosquitoes, s_{m0} , is slightly above the threshold level s_m^* ($s_{m0} = 7.5$ mosquitoes per bird); (*c,d*) to a moderate outbreak leading to 50% bird mortality at higher levels ($s_{m0} = 15$); and (*e,f*) to a severe outbreak with almost 100% bird mortality when $s_{m0} = 30$. The three simulations correspond to points *x*, *y* and *z*, respectively, in figure 3*a*.

useful graphical interpretation. For a constant mosquito population the outbreak threshold is s_m^* , but for a seasonally variable population the threshold depends on the average population level (figure 3*b,c*). We represent mosquito seasonality as a simple step function (figure 3*b*), giving the mean mosquito population over the year,

$$\bar{s}_m = (t_a s_m^a + t_b s_m^b) / (t_a + t_b), \tag{6.1}$$

where t_a and t_b are the total times spent at population levels s_m^a and s_m^b , respectively. The mean disease growth rate is then given by

$$\bar{\lambda} = (t_a \lambda_a + t_b \lambda_b) / (t_a + t_b), \tag{6.2}$$

where λ_a and λ_b are the largest eigenvalues of \mathcal{F} evaluated at s_m^a and s_m^b , respectively (equation (3.8)). This gives a geometric growth ratio for infectives over the season of $e^{\bar{\lambda}(t_a + t_b)} = e^{\lambda_a t_a} e^{\lambda_b t_b}$. Setting $\bar{\lambda} = 0$ gives the critical average mosquito level, $\bar{s}_m^* > s_m^*$, above which WN will invade a seasonally variable population (figure 3*c*). For example, when the mosquito population varies 16-fold between low and high levels, \bar{s}_m^* is approximately 1.6 times higher than

s_m^* (figure 3*b,c*). Provided that the lower mosquito population level is below s_m^* , outbreak control requires only that the higher level be reduced such that $\bar{s}_m < \bar{s}_m^*$. In other words, where mosquito populations vary seasonally, intensive spraying to reduce the higher level alone may control the disease. We therefore expect WN to be easier to control in northern more seasonal regions than in southern regions.

This graphical approach, which can be extended to additional population levels, illustrates a framework that could help to maintain mosquito populations below WN outbreak levels. Although our model indicates that local WN eradication could be achieved by intensive mosquito control, global eradication would probably be impossible since re-infection could occur through bird dispersal and migration from disease reservoirs outside the control region.

A multi-season model can be constructed from sequential iterations of the single-season model, with net bird reproduction and infectious-mosquito over-winter survival (Nasci *et al.* 2001; Turell *et al.* 2001) occurring in a single

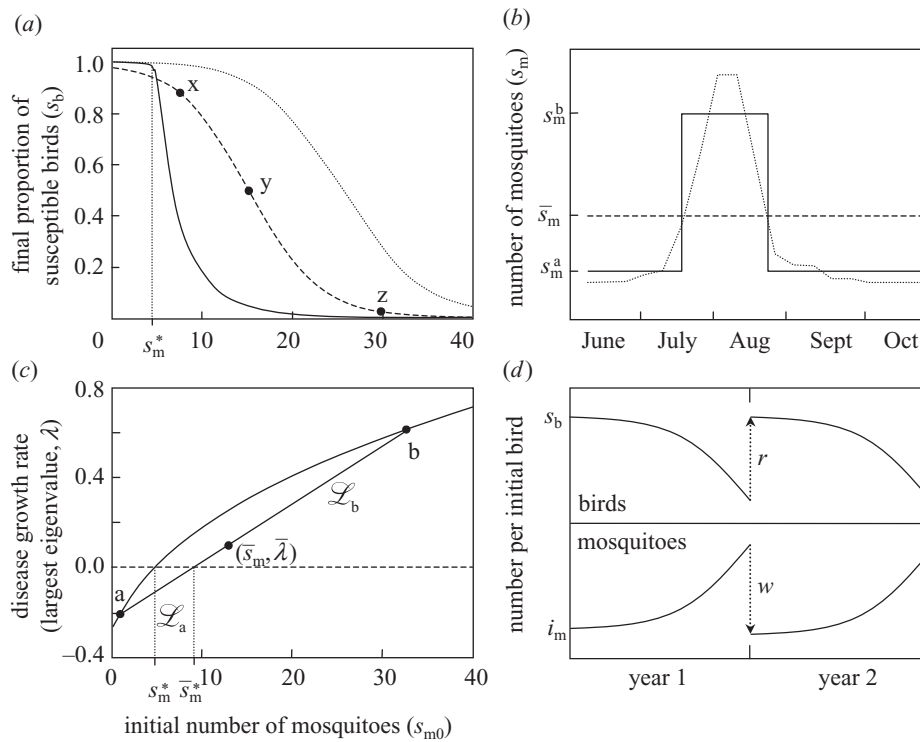


Figure 3. Control implications and temporal extensions of the WN model. (a) Constant mosquito population. Relationship between final susceptible crow population (s_b) and initial mosquito abundance (s_{m0}) as time approaches infinity for a WN inoculation of $i_{m0} = 0.001$ (solid curve), and at the end of a 147 day season for $i_{m0} = 0.001$ (dotted curve) and $i_{m0} = 0.01$ (dashed curve). As s_{m0} increases above the threshold level s_m^* , bird survival decreases asymptotically towards zero. Public health surveillance of dead crows can be related to s_m^* as follows. For $i_{m0} = 0.01$ and an observed bird mortality of 50%, a value of s_{m0} of ca. 15 may be inferred for that season (point y). For the same value of i_{m0} and a future goal of 10% bird mortality, s_{m0} would have to be reduced by ca. 70%. Points x, y and z correspond to the numerical simulations in figure 2. (b) Seasonally varying mosquito population. Natural variation in mosquito density (dotted line) from June to October in Boston, USA. Spielman's (2001) original fig. 1 data replotted here on a linear scale) can be represented crudely as a step function from s_m^a to s_m^b to s_m^a (solid line), with corresponding time periods t_a and t_b , giving a mean density, \bar{s}_m (dashed line). (c) Invasion criteria for fixed and seasonally variable mosquito populations. The relationship between the largest eigenvalue, λ , and s_{m0} is shown for a fixed population (curved line). A WN outbreak occurs when $\lambda > 0$, i.e. when $s_{m0} > s_m^*$. In a variable population, the linear relationship between the mean values $\bar{\lambda}$ and \bar{s}_m is given by the straight line, $\mathcal{L} = \mathcal{L}_a + \mathcal{L}_b$, connecting points a (s_m^a, λ_a) and b (s_m^b, λ_b). A WN outbreak occurs when $\bar{\lambda} > 0$, i.e. when $\bar{s}_m > \bar{s}_m^*$. For a given season, the point $(\bar{s}_m, \bar{\lambda})$ may be calculated from equations (6.1) and (6.2) or may be obtained graphically as the point along \mathcal{L} where the ratio between line segments $\mathcal{L}_a : \mathcal{L}_b = t_a : t_b$. (d) Multi-season extension of the WN model to time-discrete steps in which susceptible bird (s_b) reproduction occurs at rate r and infectious mosquito (i_m) over-winter survival has probability w between each iteration of the time-continuous single-season model.

time-step between seasons (figure 3d). Since the dimensionless bird populations are expressed as fractions of the initial density, each season begins with $s_b = n_b = 1$. Rescaling the fractional densities annually allows actual densities to be predicted.

This within-season model is an important first step in understanding WN dynamics and in highlighting the data needed for effective management. Our approach differs from those of previous models (Lord & Day 2001; Thomas & Urena 2001; Theophilides *et al.* 2003) in focusing on a mechanistic rather than a statistical representation of disease dynamics, and in using an analytical as well as numerical analysis.

The model will be extended biologically to additional bird species, spatially to consider bird migration and latitudinal variation in host and vector population dynamics and dispersal (Rappole *et al.* 2000; Peterson *et al.* 2003; Theophilides *et al.* 2003), and temporally as in figure 3d. The analytical methods and disease-control tools

presented here for WN can be readily applied to other complex host-vector systems.

This work was supported by a University of Alberta studentship (T.de-C.-B.), Canada Research Chair and NSERC (M.A.L.) and the Killam Trust and NSERC (M.J.W.). The authors thank H. MacIsaac for encouraging them to work on this problem, and P. van den Driessche, J. Watmough and two anonymous reviewers for their valuable comments.

REFERENCES

Anderson, J. F., Andreadis, T. G., Vossbrinck, C. R., Tirrell, S., Wakem, E. M., French, R. A., Garmendia, A. E. & Van Kruiningen, H. J. 1999 Isolation of West Nile virus from mosquitoes, crows, and a Cooper's hawk in Connecticut. *Science* **286**, 2331–2333.

Anderson, R. M. & May, R. M. 1991 *Infectious diseases of humans*. Oxford University Press.

- Bernard, K. (and 15 others) 2001 West Nile virus infection in birds and mosquitoes, New York State, 2000. *Emerging Infect. Dis.* **7**, 679–685.
- Binder, S., Levitt, A. M., Sacks, J. J. & Hughes, J. M. 1999 Emerging infectious diseases: public health issues for the 21st century. *Science* **284**, 1311–1313.
- Blower, S. M. & McLean, A. R. 1991 Mixing ecology and epidemiology. *Proc. R. Soc. Lond. B* **245**, 187–192.
- Centers for Disease Control (CDC) 2002 West Nile virus activity—United States, November 21–26, 2002. *MMWR Morbid. Mortal. Wkly Rep.* **51**, 1072–1073.
- Hayes, C. G. 1988 West Nile fever. In *The arboviruses: epidemiology and ecology*, vol. 5 (ed. T. P. Monath), pp. 59–88. Boca Raton, FL: CRC Press.
- Hayes, J. & Hsi, B. P. 1975 Interrelationships between selected meteorologic phenomena and immature stages of *Culex pipiens quinquefasciatus* Say: study of an isolated population. *J. Med. Entomol.* **12**, 299–308.
- Keeling, M. J., Woolhouse, M. E. J., Shaw, D. J., Matthews, L., Chase-Topping, M., Haydon, D. T., Cornell, S. J., Kapey, J., Wilesmith, J. & Grenfell, B. T. 2001 Dynamics of the 2001 UK foot and mouth epidemic: stochastic dispersal in a heterogeneous landscape. *Science* **294**, 813–817.
- Komar, N., Langevin, S., Hinten, S., Nemeth, N., Edwards, E., Hettler, D., Davis, B., Bowen, R. & Bunning, M. 2003 Experimental infection of North American birds with the New York 1999 strain of West Nile virus. *Emerging Infect. Dis.* **9**, 311–322.
- Langevin, S. A., Bunning, M., Davis, B. & Komar, N. 2001 Experimental infection of chickens as candidate sentinels for West Nile virus. *Emerging Infect. Dis.* **7**, 726–729.
- Lord, C. C. & Day, J. F. 2001 Simulation studies of St Louis encephalitis and West Nile viruses: the impact of bird mortality. *Vector Borne Zoonotic Dis.* **1**, 317–329.
- McLean, R. G., Ubico, S. R., Docherty, D. E., Hansen, W. R., Sileo, L. & McNamara, T. S. 2001 West Nile virus transmission and ecology in birds. *Ann. N. Y. Acad. Sci.* **951**, 54–57.
- Mogi, M., Miyagi, I. & Cabrera, B. D. 1984 Development and survival of immature mosquitoes (Diptera: Culicidae) in Philippine rice fields. *J. Med. Entomol.* **21**, 283–291.
- Mpho, M., Callaghan, A. & Holloway, G. J. 2002 Temperature and genotypic effects on life history and fluctuating asymmetry in a field strain of *Culex pipiens*. *Heredity* **88**, 307–312.
- Nasci, R. S., Savage, H. M., White, D. J., Miller, J. R., Cropp, B. C., Godsey, M. S., Kerst, A. J., Bennett, P., Gottfried, K. & Lanciotti, R. S. 2001 West Nile virus in overwintering *Culex* mosquitoes, New York City, 2000. *Emerging Infect. Dis.* **7**, 742–744.
- New York City Department of Health and Mental Hygiene 2003 Comprehensive mosquito surveillance and control plan. New York: New York City Department of Health and Mental Hygiene.
- Oda, T., Uchida, K., Mori, A., Mine, M., Eshita, M., Kurokawa, K., Kato, K. & Tahara, H. 1999 Effects of high temperature on the emergence and survival of adult *Culex pipiens molestus* and *Culex quinquefasciatus* in Japan. *J. Am. Mosq. Control Assoc.* **15**, 153–156.
- Petersen, L. R. & Roehrig, J. T. 2001 West Nile virus: a reemerging global pathogen. *Emerging Infect. Dis.* **7**, 611–614.
- Peterson, A. T., Vieglais, D. A. & Andreasen, J. K. 2003 Migratory birds modeled as critical transport vectors for West Nile virus in North America. *Vector Borne Zoonotic Dis.* **3**, 27–37.
- Rappole, J., Derrickson, S. R. & Hubalek, Z. 2000 Migratory birds and spread of West Nile virus in the Western hemisphere. *Emerging Infect. Dis.* **6**, 1–16.
- Reisen, W. K. & Siddiqui, T. F. 1979 Horizontal and vertical estimates of immature survivorship for *Culex tritaeniorhynchus* (Diptera: Culicidae) in Pakistan. *J. Med. Entomol.* **16**, 207–218.
- Reisen, W. K., Meyer, R. P., Shields, J. & Arbolante, C. 1989 Population ecology of preimaginal *Culex tarsalis* (Diptera: Culicidae) in Kern County, California. *J. Med. Entomol.* **26**, 10–22.
- Sardelis, M. R. & Turell, M. J. 2001 *Ochlerotatus j. japonicus* in Frederick county, Maryland: discovery, distribution, and vector competence for West Nile virus. *J. Am. Mosq. Control Assoc.* **17**, 137–141.
- Senne, D. A., Pedersen, J. C., Jutto, D. L., Taylor, W. D., Schmitt, B. J. & Panigrahy, B. 2000 Pathogenicity of West Nile virus in chickens. *Avian Dis.* **44**, 642–649.
- Spielman, A. 2001 Structure and seasonality of Nearctic *Culex pipiens* populations. *Ann. N. Y. Acad. Sci.* **951**, 220–234.
- Swayne, D. E., Beck, J. R., Smith, C. S., Shieh, W. J. & Zaki, S. R. 2001a Fatal encephalitis and myocarditis in young domestic geese (*Anser anser domesticus*) caused by West Nile virus. *Emerging Infect. Dis.* **7**, 751–753.
- Swayne, D. E., Beck, J. R. & Zaki, S. 2001b Pathogenicity of West Nile virus for turkeys. *Avian Dis.* **44**, 932–937.
- Theophilides, C. N., Ahearn, S. C., Grady, S. & Merlino, M. 2003 Identifying West Nile virus risk areas: the dynamic continuous-area space-time system. *Am. J. Epidemiol.* **157**, 843–854.
- Thomas, D. M. & Urena, B. 2001 A model describing the evolution of West Nile-like encephalitis in New York City. *Math. Comput. Model.* **34**, 771–781.
- Turell, M. J., O'Guinn, M. & Oliver, J. 2000 Potential for New York mosquitoes to transmit West Nile virus. *Am. J. Trop. Med. Hyg.* **62**, 413–414.
- Turell, M. J., O'Guinn, M. L., Dohm, D. J. & Jones, J. W. 2001 Vector competence of North American mosquitoes (Diptera: Culicidae) for West Nile virus. *J. Med. Entomol.* **38**, 130–134.
- van den Driessche, P. & Watmough, J. 2002 Reproduction numbers and sub-threshold endemic equilibria for compartmental models of disease transmission. *Math. Biosci.* **180**, 29–48.
- Walter, N. M. & Hacker, C. S. 1974 Variation in life table characteristics among three geographic strains of *Culex pipiens quinquefasciatus*. *J. Med. Entomol.* **11**, 541–550.
- Work, T. H., Hurlbut, H. S. & Taylor, R. M. 1955 Indigenous wild birds of the Nile delta as potential West Nile virus circulating reservoirs. *Am. J. Trop. Med. Hyg.* **4**, 872–888.

As this paper exceeds the maximum length normally permitted, the authors have agreed to contribute to production costs.